INVESTIGATION OF IRON ALUMINIDE WELD OVERLAYS

J.R. Regina, J.N. DuPont, and A.R. Marder

Materials Science and Engineering
Lehigh University
Bethlehem, PA 18015

INTRODUCTION

Corrosion and subsequent waterwall wastage has been a significant problem for coal-burning power companies since low NOx burner conditions have been implemented in their furnaces. In order to reduce the amount of waterwall corrosion, coatings for the boiler tubes, such as weld overlay claddings, are currently being pursued. Iron-aluminum based coatings are presently being studied as possible coating candidates due to their excellent corrosion resistance in high-temperature oxygen and sulfur bearing environments[1-4]. In addition, iron-aluminum based alloys are advantageous to other possible coating candidates because they are cheaper than stainless steel or Ni-based superalloys and do not demonstrate microsegregation of alloying elements unlike Ni-based superalloys[1,5]. Unfortunately, iron-aluminum weld overlay claddings are susceptible to hydrogen cracking at aluminum contents greater than 10wt%Al[5]. It has previously been shown that the corrosion resistance of iron-aluminum alloys is directly related to the aluminum content of the alloy[3,6]. Therefore, chromium was added to iron-aluminum alloys to determine if they promoted the corrosion resistance in several corrosive environments.

In low NOx furnace environments two types of corrosion can occur that greatly govern the corrosion behavior of the coating. During the initial furnace startup, gaseous corrosion can occur when exposed metal comes in contact with the aggressive gas. After extended furnace operation, un-burnt coal particles, ash, and gaseous corrosion products can adhere to the boiler tube wall. Under these conditions gas-slag corrosion takes place, where solid-state reactions between the slag and metal can accelerate the corrosion rates. Therefore, two types of corrosion tests were used to simulate low NOx corrosive environments. Gaseous corrosion testing was used to determine the corrosion kinetics of alloys exposed to aggressive sulfidizing, oxidizing, and mixed sulfidizing/oxidizing gases. Gas-slag corrosion tests were used to determine the corrosion behavior of an alloy in contact with sulfur bearing powder.

EXPERIMENTAL PROCEDURE

Alloys were made by arc-melting high purity components under an argon atmosphere and drop cast into a water-cooled copper mold. Cast alloys were used because it was previously shown that the high temperature corrosion behavior of weld overlays could be explained by using cast alloys of equivalent composition[7]. Alloys used in the study contained 7.5wt% or 10wt% carried out using a Netzsch STA 409 high-temperature thermogravimetric (TG) balance, which measures changes in weight over time. Samples were ground to 600 grit and measured to the nearest hundredth of a millimeter. They were then weighed to the nearest tenth of a milligram using a digital balance and cleaned using acetone. The specimens were heated at a rate of 50°C/min and were held at 500°C for 100 hours. Water vapor present in the mixed oxidizing/sulfidizing and the oxidizing environments was injected into the furnace at a controlled rate. The three gas compositions used for this study can be seen in Table 2. The sulfur and oxygen partial pressures were calculated for the gases using the HSC Chemistry computer program[8]. Selected exposed

samples were cut approximately 80% through and submersed into liquid N_2. The samples were then cracked and dropped into ethanol to obtain cracked surface images. A JEOL 6300 Scanning Electron Microscope (SEM) was used to obtain surface images as well as images of cracked cross sections. Samples were observed with a 17mm working distance and accelerating voltages of 5keV and 10keV. Energy-Dispersive Spectroscopy (EDS) was used to identify the corrosion products that were observed on samples. SEM surface images were used with an imaging program to obtain area fractions.

Table 1– Alloy compositions used for corrosion testing. All values are in weight percent.

Alloy Designation	Fe	Al	Cr
Fe-7.5Al	Bal.	7.38	--------
Fe-7.5Al-1Cr	Bal.	7.45	0.96
Fr-7.5Al-2Cr	Bal.	7.59	2.09
Fe-7.5Al-5Cr	Bal.	7.77	5.03
Fe-10Al	Bal.	10.04	--------
Fe-10Al-1Cr	Bal.	10.04	0.99
Fe-10Al-2Cr	Bal.	10.19	2.16
Fe-10Al-5Cr	Bal.	10.74	5.18

Table 2– Gas Compositions used for corrosion testing (vol. %).

Gas Component	Sulfidizing Gas	Mixed Oxidizing/Sulfidizing Gas	Oxidizing Gas
O_2	--------	--------	2
CO	15	10	--------
CO_2	--------	5	15
H_2	3	--------	--------
H_2O	--------	2	6
H_2S	0.12	0.12	--------
SO_2	--------	--------	0.12
N_2	Bal.	Bal.	Bal.
Log Po_2	-28	-19	-2
Log Ps_2	-6	-8	-46

Gas-slag corrosion experiments[9] were conducted using a Lindberg/Blue Horizontal Tube Furnace. The samples were ground to 600 grit and cleaned using acetone. The setup consisted of a quartz ring being super-glued onto the top of the ground surface. A predetermined amount (1680mg) of FeS_2 powder, supplied by American Minerals, was poured into the quartz ring without being packed and this setup was placed into the furnace. A schematic for the gas-slag-metal samples can be seen in Figure 1. Either the oxidizing gas or the mixed oxidizing/sulfidizing gas was then introduced into the furnace at a flow of 50mL/min. The samples were heated at a rate of 50°C/min and were held at 500°C for 100 hours. Water vapor present in both gases was injected into the furnace at a controlled rate. Samples were carefully mounted in cold setting epoxy and their polished cross sections were observed using Light Optical Microscopy (LOM). LOM images were taken with an integrated camera on a LECO digital imaging system. The internal corrosion products observed in non-protective alloys were measured using an imaging program interfaced with a Light Optical Microscope.

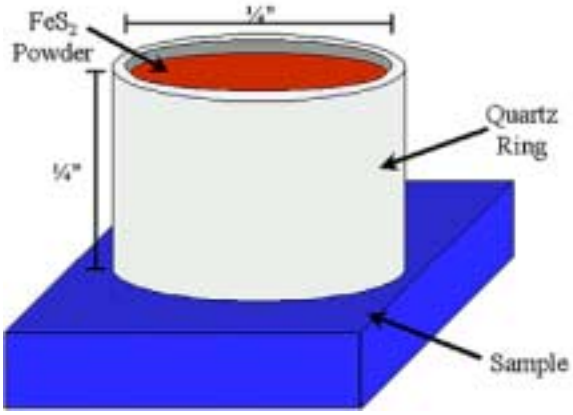

Figure 1 – Schematic diagram of the gas-slag-metal experimental setup.

RESULTS AND DISCUSSION

Gaseous Corrosion Testing

Corrosion kinetics were obtained for alloys exposed to the sulfidizing gas and can be seen in Figure 2. The alloys containing 7.5wt%Al (Figure 2a) demonstrated accelerated weight gains when containing 0-2wt%Cr, but appeared completely protective when 5wt%Cr was added to the alloy. Corrosion products that formed on the non-protective alloys were block-like in appearance and were identified as iron-sulfides (Figure 3a). On the other hand, all of the alloys containing 10wt%Al were protective during 100 hours of exposure regardless of the chromium content. All alloys containing 10wt%Al and the Fe-7.5Al-5Cr alloy maintained a thin passive layer that provided corrosion protection (Figure 3b).

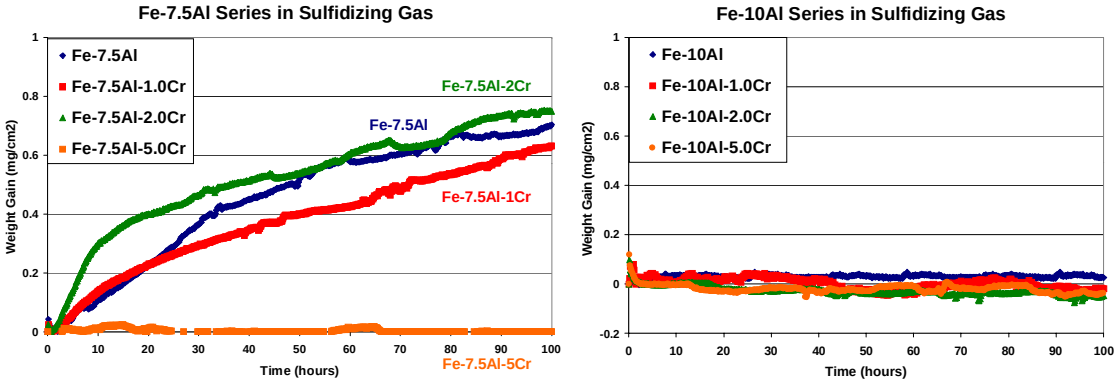

Figure 2 – Kinetic results for alloys exposed to the sulfidizing gas for 100 hours.

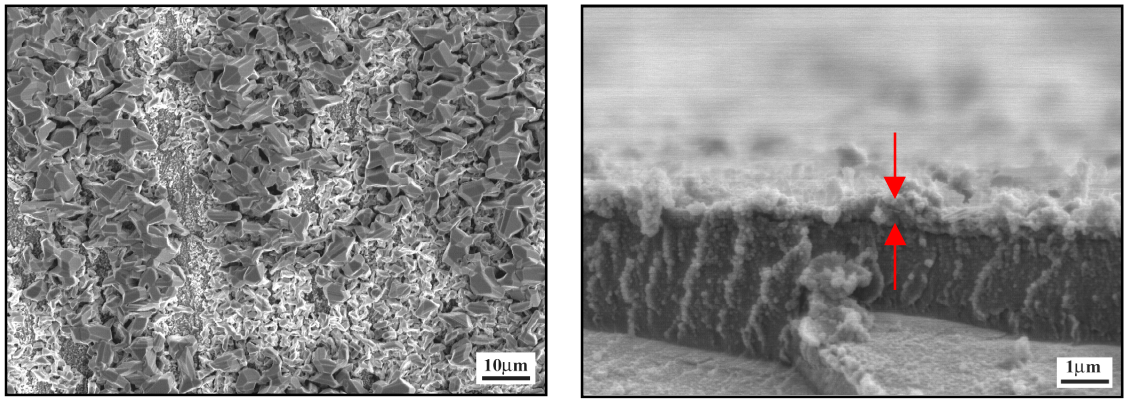

(a) **(b)**

Figure 3 – Iron sulfide corrosion product that formed on non-protective alloys (a) and the passive layer that was maintained on protective alloys (b).

Kinetic results from selected alloys exposed to the oxidizing environment can be seen in Figure 4a. It can again be seen that alloys containing 7.5wt%Al required at least 5wt%Cr in order to demonstrate a sharp reduction in the corrosion kinetics. Alloys containing 10wt%Al appeared to be completely protective during 100 hours of exposure to the oxidizing gas despite the chromium content in the alloy. When considering the corrosion product morphology, non-protective samples were covered with round-like corrosion nodules that were identified to be rich in iron and oxygen (Figure 4b). Some alloys, such as Fe-7.5Al, formed plate-like nodules above the round nodules once the round nodules completely overgrew and covered the sample surface. Protective alloys formed a passive layer that was successfully maintained during 100 hours of exposure. The passive layer was again less than 1μm thick and can also be seen in Figure 4b.

Alloys containing 7.5wt%Al that were exposed to the mixed oxidizing/sulfidizing gas gained a significant amount of weight regardless of the amount of chromium contained in the alloy (Figure 5a). These non-protective alloys formed thick, block-like scales that completely covered the sample surface and significantly cracked when the samples were removed from the furnace (Figure 5b). These corrosion products were found to be rich in iron and sulfur and their block-like morphology was consistent with the iron sulfide corrosion products that formed on several samples exposed to the sulfidizing gas. The binary alloy Fe-10Al showed a reduction in total weight gain when compared to the alloys containing 7.5wt%Al, but the corrosion kinetics were completely suppressed when chromium was added to the alloy (Figure 6a). Again the protective alloys all formed a thin passive oxide layer that was observed to be less than 1μm thick (Figure 6b).

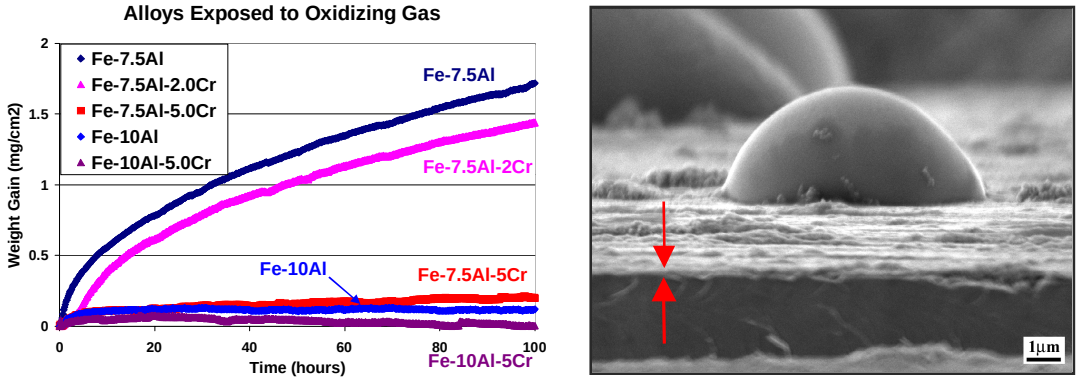

Figure 4 – Corrosion kinetics for alloys exposed to the oxidizing gas (a) and the round-like nodules that formed on non-protective samples (b). Note the thin oxide layer designated by arrows in (b) is the passive layer that remains completely intact for protective alloys.

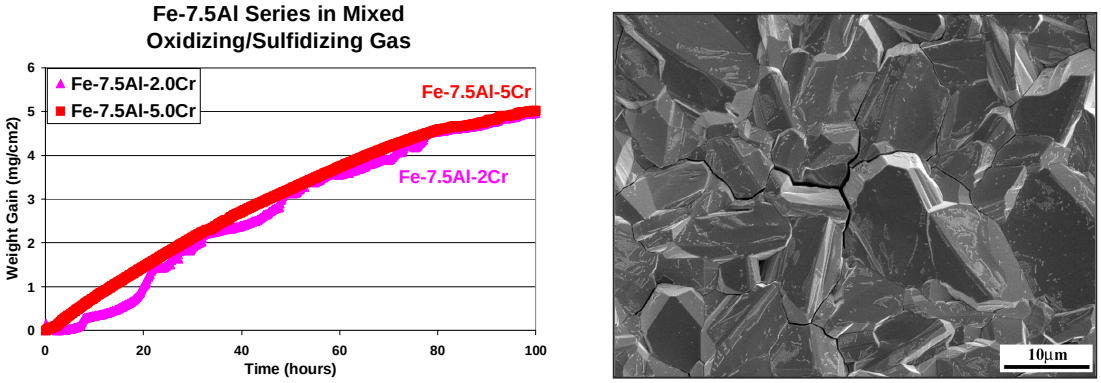

Figure 5 – Corrosion kinetics for select alloys containing 7.5wt%Al that were exposed to the mixed oxidizing/sulfidizing environment (a), and the thick block-like corrosion product that covered the non-protective alloys.

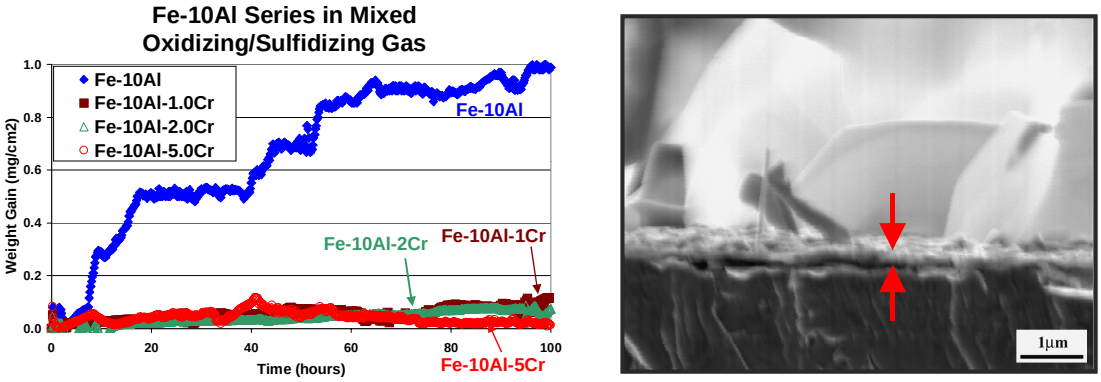

Figure 6 – Corrosion kinetics for alloys containing 10wt%Al that were exposed to the mixed oxidizing/sulfidizing gas (a), and the passive layer that formed on protective alloys (b).

Gas-Slag Corrosion Testing

Selected cross sections of alloys containing 7.5wt%Al exposed to the oxidizing gas while in contact with FeS_2 powder can be seen in Figure 7. All of the alloys containing 7.5wt%Al exposed to this environment developed thick external corrosion layers, which were at least 100μm thick, as well as uniform substrate corrosion scales that penetrated into the alloy. The external corrosion scale seemed to consist of two distinct layers. The layer directly adjacent to the metal substrate was observed to contain a large amount of porosity while the outer layer of the external scale was a thick solid layer that contained relatively no pores. The substrate corrosion products observed on these alloys seemed to consist of multiple layers and cracks could be seen to run through the substrate corrosion products perpendicular to the substrate/external corrosion scale interface. These cracks can act as fast pathways for corrosion to take place and are therefore very detrimental to the corrosion resistance of the alloy.

Thickness measurements were taken of the internal substrate corrosion scales in these alloys to determine if chromium additions had any significant affect on the corrosion behavior. The substrate corrosion scale thickness measurements for alloys containing 7.5wt%Al that were exposed to the oxidizing gas can be seen in Table 3. The thickness measurements showed that there was no significant effect of chromium on the substrate scale thickness until 5wt%Cr was added. It was also observed that cracking of the substrate corrosion scale occurred in all samples containing thickness layers in excess of approximately 45μm. The external corrosion layer thickness seemed to decrease slightly with the addition of chromium, but the scales were too convoluted to obtain relevant thickness data. Regardless of the chromium concentration, alloys containing 10wt%Al were completely protective when exposed to the oxidizing gas while in contact with the FeS_2 powder. These samples were observed to form neither an external corrosion layer nor an internal substrate corrosion layer.

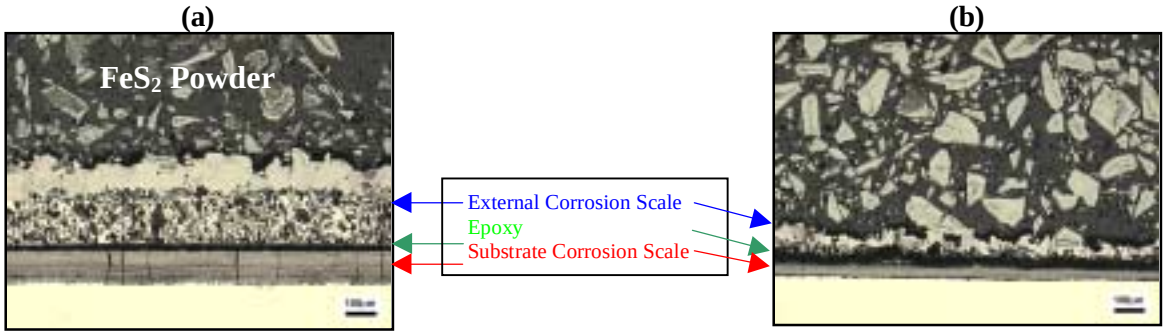

Figure 7 – Cross sectional view of Fe-7.5Al (a) and Fe-7.5Al-5Cr (b) exposed to the oxidizing gas while in contact with FeS_2 powder.

Table 3 – Substrate corrosion layer thickness for samples exposed to FeS_2 powder and the oxidizing environment.

Alloy	Thickness (μm)	Standard Deviation
Fe-7.5Al	103.1	12.5
Fe-7.5Al-1Cr	69.2	2.0
Fe-7.5Al-2Cr	91.3	1.6
Fe-7.5Al-5Cr	43.3	2.0

Representative polished cross section of alloys containing 7.5wt%Al exposed to the mixed oxidizing/sulfidizing gas and FeS_2 powder can be seen in Figure 8. It was found that Fe-7.5Al, Fe-7.5Al-1Cr, and Fe-7.5Al-2Cr, all formed significant substrate and external corrosion scales after 100 hours of exposure. The external corrosion layers formed on these alloys were fairly non-uniform and appeared to be several microns thick. The substrate corrosion products formed on these alloys were uniform and appeared to be made up of multiple corrosion layers (Figure 8a). Fe-7.5Al-5Cr formed a significant substrate scale, similar to the aforementioned alloys, but formed a very thin external corrosion layer (Figure 8b). All alloys containing 10wt%Al tested in the mixed oxidizing/sulfidizing environment and in contact with FeS_2 showed no signs of corrosion after 100 hours of exposure.

Thickness measurements were again taken of the substrate corrosion scales present on the alloys containing 7.5wt%Al (Table 4). As can be seen from this table, some measured improvement to the substrate scale thickness was made only when 5wt%Cr was added. Although no measurements were made of the external corrosion product thickness, similar results were observed. From these cross-sectional observations, it can be seen that chromium additions of 1-2wt% may have made a slight improvement on the external corrosion layer thickness, but significant improvement occurred when 5wt%Cr was added.

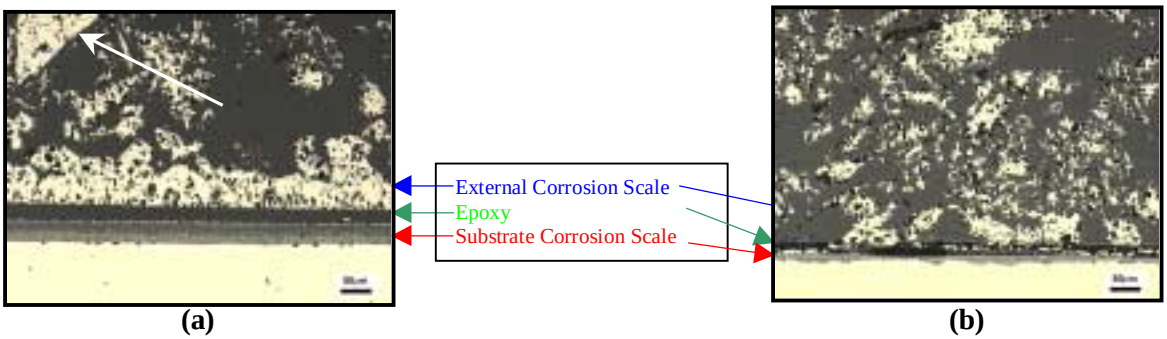

Figure 8 – Cross sectional view of Fe-7.5Al (a) and Fe-7.5Al-5Cr (b) exposed to the mixed oxidizing/sulfidizing gas while in contact with FeS_2 powder.

Table 4 – Substrate corrosion scale thickness for samples exposed to FeS_2 powder and the mixed oxidizing/sulfidizing environment.

Alloy	Thickness (μm)	Standard Deviation
Fe-7.5Al	30.5	2.1
Fe-7.5Al-1Cr	19.7	4.3
Fe-7.5Al-2Cr	26.3	2.8
Fe-7.5Al-5Cr	11.3	1.8

Results from the gaseous corrosion testing and the gas-slag corrosion testing clearly show that an increase in aluminum concentration increases the corrosion resistance of an iron-aluminum alloy. It can be seen that additions of chromium up to 5wt% help to improve the corrosion behavior of iron-aluminum alloys. To help quantify the effect of aluminum and chromium on the corrosion behavior, multiple linear regression analysis was performed on the data collected from both types of corrosion experiments. It was found that aluminum was approximately twice as effective as chromium at decreasing the total weight gain that occurred during 100 hours of exposure in the gaseous corrosion environments. Similarly, aluminum was approximately twice as effective as chromium at decreasing the substrate corrosion scale thickness that formed on samples exposed

to the gas-slag corrosive environments. Through this relationship, an alloying content factor was created to numerically represent both the aluminum and chromium concentration and to help determine the effect of composition on the corrosion resistance in these test environments. The alloying content factor (ϕ) was found to be:

$$\phi = (wt\%Al) + 0.5(wt\%Cr) \quad (1)$$

Values of ϕ for each alloy used in this study can be seen in Table 5.

Table 5 – Alloying content factor (ϕ) for each alloy used in the study.

Alloy Designation	Al	Cr	ϕ = (wt%Al) + 0.5(wt%Cr)
Fe-7.5Al	7.38	--------	**7.4**
Fe-7.5Al-1Cr	7.45	0.96	**7.9**
Fe-7.5Al-2Cr	7.59	2.09	**8.6**
Fe-7.5Al-5Cr	7.77	5.03	**10.3**
Fe-10Al	10.04	--------	**10.0**
Fe-10Al-1Cr	10.04	0.99	**10.5**
Fe-10Al-2Cr	10.19	2.16	**11.3**
Fe-10Al-5Cr	10.74	5.18	**13.3**

The total weight gain for each alloy tested was plotted against ϕ in order to determine the critical alloying content required for protection in the various gaseous corrosion environments. The critical alloying content required to prevent any weight gain in each of the three atmospheres can be seen in Figure 9. It can be seen from these figures that a critical alloying content of approximately 10 was required to significantly reduce the corrosion kinetics and the total weight gain during 100 hours of exposure. In order to completely suppress any measurable weight gain during 100 hours of exposure, an alloying content of approximately 12.5 is required. When considering the amount of internal substrate corrosion that occurred for samples exposed to the gas-slag corrosive environments, similar results were found. The critical alloying content needed to prevent any internal corrosion from occurring was 10 in both gas-slag corrosive environments.

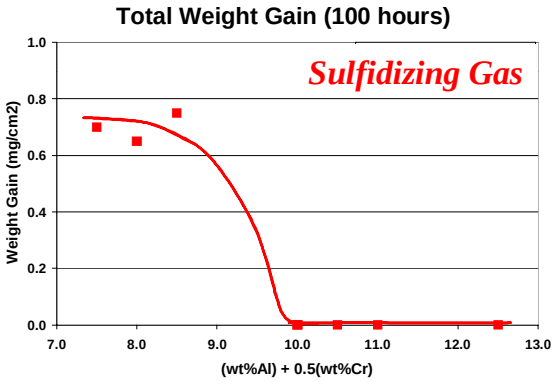

(a)

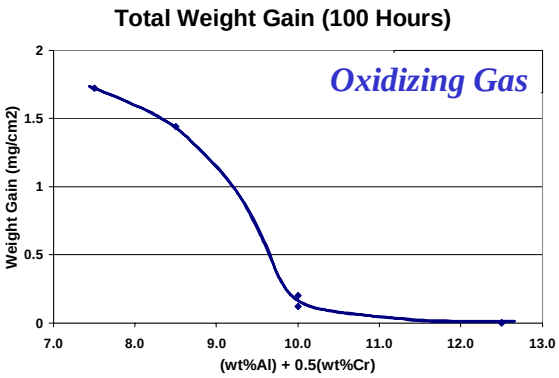

(b)

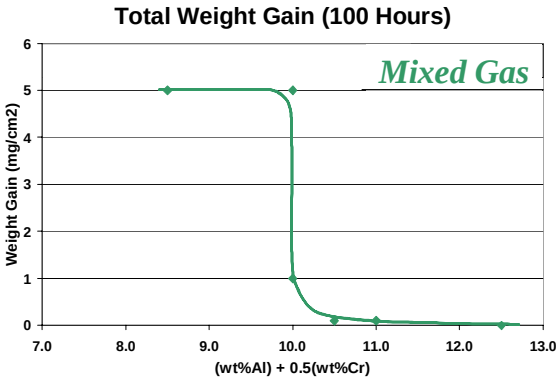

(c)

Figure 9 – Critical alloying content needed to significantly reduce the total weight gain during 100 hours of exposure in the sulfidizing gas (a), the oxidizing gas (b), and the mixed oxidizing/sulfidizing atmosphere (c).

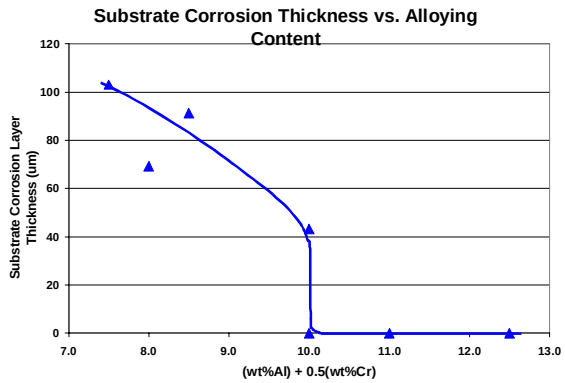

(a)

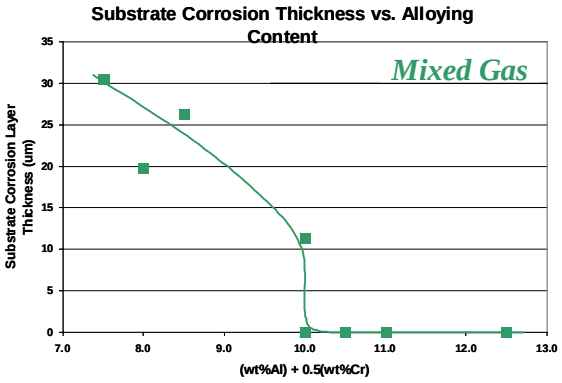

(b)

Figure 10 – Critical alloying content needed to significantly reduce the thickness of the internal substrate corrosion layer that formed on samples during 100 hours of exposure in the oxidizing gas (a) and the mixed oxidizing/sulfidizing atmosphere (b).

CONCLUSIONS

- Chromium additions helped increase corrosion resistance for Fe-Al alloys exposed to all tested corrosion environments.

- Alloying Content Factor of:
  $$AC = (wt\%Al) + 0.5(wt\%Cr)$$
  was developed for Fe-Al-Cr alloys exposed in this study.

- Alloying content factor (ϕ) of 10 was required to prevent large weight gains during gaseous corrosion testing and significant substrate corrosion during gas-slag corrosion testing.

- Alloying Content of 12.5 (Fe-10Al-5Cr) was needed to completely suppress unwanted corrosion products from forming during exposure to the gaseous environments.

REFERENCES

1. C. G. McKamey, J. H. DeVan, P. F. Tortorelli, and V. K. Sikka. *J. Mater. Res.* **6**, pp. 1779-1805 (1991).

2. J. H. DeVan and P. F. Tortorelli. *Mater. High Temp.* **11**, pp. 30-35 (1993).

3. P. F. Tortorelli, J. H. DeVan, G. M. Goodwin, and M. Howell. (1995). *In Elevated Temp. Coat.: Sci. Technol. I, Proc. Symp.* pp. 203-12, Rosemont, IL, Oct 3-6, TMS, Warrendale, PA.

4. S. W. Banovic, J. N. DuPont, and A. R. Marder. (1999). *In Corrosion 99*, pp. 12-20, Houston, TX, April 25, National Association of Corrosion Engineers.

5. S. W. Banovic, J. N. DuPont, P. F. Tortorelli, and A. R. Marder. *Weld. Res. (Miami)* **78**, pp. 23S-30S (1999).

6. S. W. Banovic, J. N. DuPont, and A. R. Marder. *Metall. Mater. Trans. A* **31A**, pp. 1805-1817 (2000).

7. P. F. Tortorelli, G. M. Goodwin, M. Howell, and J. H. DeVan. (1995) *In Heat-Resist. Mater. II*, Conf. Proc. Int. Conf., 2nd. Oak Ridge, TN.

8. HSC. HSC Chemistry for Windows, Version 4.0. (1997). Oy, Finland, Outokupmu

9. K. Luer. Investigation of Gas-Deposit-Alloy Corrosion Interactions in Simulated Combustion Environments. (2000). Dissertation, Lehigh University.